THE ASTROPHYSICAL JOURNAL, 607:L111–L114, 2004 June 1

ROSAT AND *ASCA* OBSERVATIONS OF A NARROW-LINE SEYFERT 1 GALAXY RX J0136.9−3510: BLUESHIFTED Fe Kα LINE AND EXTENDED SOFT X-RAY EMISSION

KAJAL K. GHOSH,[1] DOUGLAS A. SWARTZ,[1] ALLYN F. TENNANT,[2] KINWAH WU,[3] AND BRIAN D. RAMSEY[2]
Received 2004 March 31; accepted 2004 April 21; published 2004 April 30

ABSTRACT

RX J0136.9−3510 is an unusual narrow-line Seyfert 1 galaxy (NLS1). We have detected extended (∼12″ or ∼54 kpc at the source frame) soft X-ray emission in the *ROSAT* High Resolution Imager image, accounting for 20% of the total emission. We have also detected a highly blueshifted (7.6 keV in the source frame) Fe K α line in the *ASCA* Solid-State Imaging Spectrometer spectrum. This is the first detection of such a highly blueshifted emission line in a NLS1. Near-IR and far-IR studies indicate the presence of a possible starburst component in this NLS1. Physical models of the accretion and/or outflow and of the evolution of this NLS1 are discussed in the context of these results.

Subject headings: galaxies: active — galaxies: individual (RX J0136.9−3510) — galaxies: nuclei — galaxies: Seyfert — X-rays: galaxies

1. INTRODUCTION

Narrow-line Seyfert 1 galaxies (NLS1s) are active galactic nuclei (AGNs) having Hβ emission-line FWHMs of less than 2000 km s^{-1} and [O III]/Hβ flux ratios of less than 3.0 (Osterbrock & Pogge 1985; Goodrich 1989). NLS1s are often strong Fe II emitters and often have large amounts of dense, low-ionization, line-emitting gas in their broad-line regions (Wills et al. 1999; Kuraszkiewicz et al. 2000). It has been suggested that NLS1s are very young objects (Grupe 1996; Mathur 2000), have supersolar metallicity, are in the early stage of evolution (Grupe 1996; Mathur 2000; Mathur et al. 2001), and have evolutionary processes different from broad-line Seyfert 1 galaxies (BLS1s; Brandt et al. 1997a; Mathur et al. 2001).

Spectral indices of the X-ray spectra of NLS1s are steeper than those of BLS1s and are anticorrelated with the Hβ line width (Puchnarewicz et al. 1992; Boller et al. 1996; Brandt et al. 1997a, 1997b; Reeves & Turner 2000). A soft X-ray excess is more prominent and frequent in NLS1s (Reeves & Turner 2000; Vaughan et al. 1999; Leighly 1999a). They have significantly bluer optical and UV spectra, and they have more pronounced big blue bumps than BLS1s (Grupe et al. 1998). It has been suggested that thermal emission from the accretion disk is the origin of the soft X-ray emission (Leighly 2000). NLS1s are more variable in X-rays than are BLS1s (Boller 2000), which may be due to the beaming effect (Boller et al. 1997; Brandt et al. 1999), although this scenario has been brought into question (Leighly 1999b, 2000). Recently, Brandt & Gallagher (2000) have suggested that an evolutionary connection may be present between the luminous NLS1s and the broad absorption line quasars (BALQs). However, signatures of strong outflows have not yet been conclusively detected in the spectra of NLS1s (Leighly et al. 1997; Nicastro et al. 1999; Netzer 2000).

From the *ROSAT* and the *ASCA* observations of RX J0136.9−3510, we have detected extended soft X-ray emission and a highly blueshifted Fe Kα emission line in this galaxy, and these results are presented here.

2. IS RX J0136.9−3510 AN UNUSUAL NLS1?

RX J0136.9−3510 [R.A. = 01^{h}36^{m}54^s.45 and decl. = −35°10′53″.3 (2000), with a redshift $z = 0.289$] was detected as a bright source during the *ROSAT* All Sky Survey (RASS, with an exposure for 404 s with 0.49 ± 0.04 counts s^{-1}). The optical spectrum of this object shows that the Fe II/[O III] ratio is ∼37.2, the [O III]/Hβ flux ratio is ∼0.23, the Fe II/Hβ flux ratio is ∼8.3, and the FWHM of the Hβ line in RX J0136.9−3510 is ∼1320 km s^{-1} (Grupe et al. 1999; the FWHM of the broad component of the Hβ line of RX J0136.9−3510 is ∼2354 ± 300 km s^{-1}, based on the Gaussian profile fitting to the broad component of the Hβ line). These last two quantities are consistent with those of all 59 NLS1s in the catalog of Véron-Cetty et al. (2001).

The average Fe II/Hβ flux ratio for the 59 NLS1s in the catalog of Véron-Cetty et al. (2001) is 1.0, and that for RX J0136.9−3510 is ∼8.3. This suggests that RX J0136.9−3510 is a very strong Fe II emitter compared with other known NLS1s. These results show that RX J0136.9−3510 is an unusual NLS1 object.

3. OBSERVATIONS, DATA ANALYSIS, AND RESULTS

ROSAT High Resolution Imager (HRI) pointed observations of RX J0136.9−3510 were carried out during 1997 December 26–28 with a 30,692 s effective exposure (with count rate of ∼0.111 ± 0.002 counts s^{-1}). It is known that the residual errors in the *ROSAT* HRI aspect solution gave rise to elongated images (Zombeck et al. 1995), and this made the radial profile extended with respect to the point-spread function (PSF; David et al. 1995). We have corrected the bad aspect times in the *ROSAT* HRI image of RX J0136.9−3510 using the off-line FTOOLS HRI aspect fix script.[4] The software package LEXTRCT, locally developed (A. F. Tennant), was used to generate the background-subtracted radial profile of this image shown in Figure 1. For comparison, the new improved *ROSAT* HRI PSF profile[5] is also shown in Figure 1, which was scaled vertically to match the data count rate at the maximum of the observed radial profile of the NLS1.

[1] Universities Space Research Association, NASA/Marshall Space Flight Center (MSFC)/National Space and Technology Center (NSSTC), Mail Code SD 50, Huntsville, AL 35805; kajal.ghosh@msfc.nasa.gov, doug.swartz@msfc.nasa.gov.
[2] Space Science Department, NASA/MSFC/NSSTC, Mail Code SD 50, Huntsville, AL 35805; tennant@alph.msfc.nasa.gov, brian.ramsey@msfc.nasa.gov.
[3] Mullard Space Science Laboratory, University College of London, Holmbury St. Mary, Dorking, Surrey RH5 6NT, UK; kw@mssl.ucl.ac.uk

[4] See http://hea-www.harvard.edu/rosat/aspfix.html.
[5] See http://rosat.gsfc.nasa.gov/docs/rosat/ruh/handbook/node109.html.

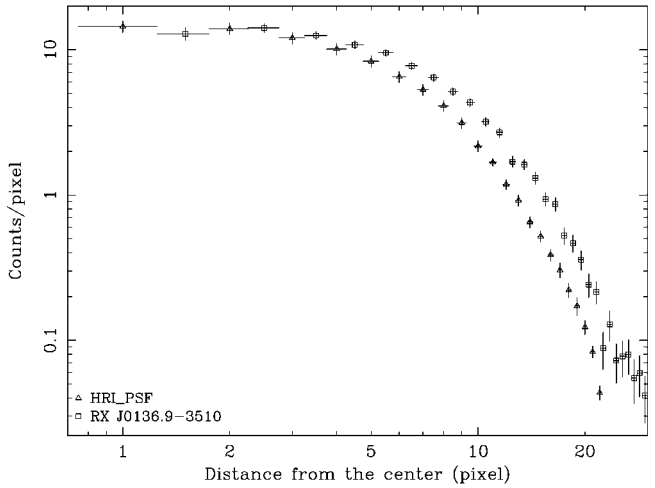

FIG. 1.—Radial profiles of the *ROSAT* HRI image of RX J0136.9−3510 (*crosses*) and the new improved *ROSAT* HRI PSF (*triangles*).

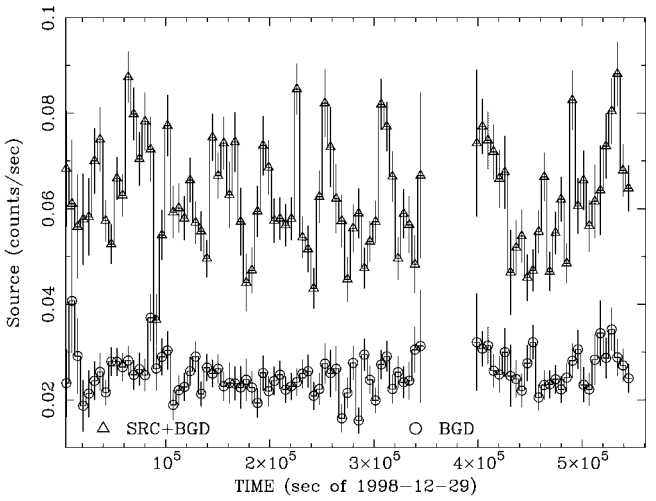

FIG. 2.—*ASCA* SIS0 light curve (the triangles represent source+background, and the circles represent background) of RX J0136.9−3510, observed between 1998 December 28 and 1999 January 4 with a 195 ks effective exposure (5400 s binning).

Inspection of Figure 1 shows that systematic extended emissions are present beyond ~5″ radius from the center of this NLS1. This extended emission component is roughly ~20% of the total HRI emission. At the source frame, this emission component is extended up to 55 kpc (12″). The HRI light curve of RX J0136.9−3510 shows weak variability of this source.

The RASS spectrum of this source and the corresponding background spectrum were extracted using the LEXTRCT program. The source spectrum was binned so that there are at least 20 photons bin^{-1}. The *ROSAT* PSPC response matrix was obtained from the HEASARC database, and the ARF file was created using FTOOLS version 5.1A. The XSPEC version 11.2 package was used for the spectral analysis, with the absorption cross sections of Balucinska-Church & McCammon (1992) for the Galactic absorptions. The redshifted blackbody (BB; $kT_{\rm BB} = 42 \pm 6$ eV) or the Raymond-Smith (RS; $kT_{\rm RS} = 81 \pm 7$ eV) or the power-law (PL; $\Gamma = 3.4 \pm 0.15$) models, modified by the Galactic absorption (GA; $N_{\rm H} = 1.79 \times 10^{20}$ cm^{-2}), fit the RASS spectrum of RX J0136.9−3510 equally well ($\chi^2_r \sim 0.5$ for 6 degrees of freedom [dof]). The errors quoted in this Letter were computed for the 90% confidence level ($\chi^2_{\rm min} + 2.71$). The steep power law may be an indication of the presence of soft excesses in this NLS1, which is further indicated by the presence of the extended (10″–12″) X-ray emission in the *ROSAT* HRI image of this object (Fig. 1). The model-computed flux of RX J0136.9−3510 during the RASS observations was $(2.78 \pm 0.33) \times 10^{-12}$ ergs cm^{-2} s^{-1}, in the *ROSAT* band.

ASCA observations of RX J0136.9−3510 were carried out between 1998 December 28 and 1999 January 4, with accumulated Gas Imaging Spectrometer (GIS) and Solid-State Imaging Spectrometer (SIS) exposures of 135,552 and 195,037 s, respectively. *ASCA* GIS2, GIS3 and SIS0, SIS1 count rates (background-subtracted) are 0.046 and 0.023 counts s^{-1}, respectively, and the GIS data were too noisy for analysis. SIS0 light curves (of the source and the background) of this NLS1 were extracted using LEXTRCT and are shown in Figure 2 with 5400 s binning (~1 orbit of the satellite). It can be seen from Figure 2 that RX J0136.9−3510 displayed irregular variability during the *ASCA* SIS0 observations. Characterization of the variability in an irregularly sampled light curve can be done by computing the excess variance parameter (Tennant & Mushotzky 1983). This parameter ($\sigma^2_{\rm rms}$) and its error were computed for the background-subtracted *ASCA* SIS0 light curve binned at 5400 s (to achieve a reasonable signal-to-noise ratio) using the relations given by Nandra et al. (1997). The computed value of $\sigma^2_{\rm rms}$ is $(8.75 \pm 0.06) \times 10^{-2}$, which suggests that the total (soft plus hard) flux varied by ~29%. We also performed a χ^2 test against a constant flux hypothesis of the *ASCA* SIS0 light curve of RX J0136.9−3510, and the result shows that the light curve is variable ($\chi^2_r = 2.94$ for 27 dof). The values of $\sigma^2_{\rm rms}$ and the observed 2–10 keV luminosity of RX J0136.9−3510 are consistent for an NLS1 (see Figs. 3 and 8 of Leighly 1999a). The computed mass of the black hole of RX J0136.9−3510 is $4 \times 10^7\ M_\odot$ using equation (4) of Nikolajuk et al. (2004) and the value of $\sigma^2_{\rm rms}$. Both the soft (0.5–2.0 keV) and the hard (2–10 keV) fluxes varied during the *ASCA* SIS0 observations, with the fractional variability in the soft band being larger (~36.7%) than that seen in the hard band (~14.5%).

The source and the corresponding background spectra from the SIS detectors were also extracted using LEXTRCT. The SIS spectra were binned with a minimum of 30 photons bin^{-1}. *ASCA* SIS response matrices and the GIS and SIS ARF files were created using FTOOLS version 5.1A. The efficiency losses of the SIS detectors were parameterized following the prescription given by Yaqoob et al. (2000). SIS0 and SIS1 spectra of RX J0136.9−3510 were fitted simultaneously. Both the spectra in the energy range 2.0–8.0 keV at the observer's frame were fitted with the redshifted absorption-corrected power-law model with an additional fixed absorption parameter ($N_{\rm H} = 9.0 \times 10^{20}$ cm^{-2}) to compensate for the low-energy efficiency losses of the SIS detectors (this parameter will be used as a fixed parameter throughout the analysis). From this, we found that the fitted value of the hydrogen column density ($N_{\rm H}$) becomes zero. We therefore fixed the value of $N_{\rm H}$ to the Galactic value (1.79×10^{20} cm^{-2}) and refitted the spectra with this model (Table 1). The value of Γ obtained from this fit in the 2.0–8.0 keV band was 2.3 ± 0.1. This value of Γ was then fixed to fit both the SIS spectra in the 0.7–8.0 keV range ($\Gamma = 2.99 \pm 0.08$, when left free). The data and model (*top panel*) and the ratio between the data and the model (*bottom panel*) are shown in Figure 3. It can be seen from this figure that there are two spectral features: (1) an excess emission below 1 keV (soft X-ray excess) and (2) an emission line around 5.9 keV. The RS ($kT_{\rm RS} = 0.2 \pm 0.03$ keV) or the BB

TABLE 1
THE BEST-FIT SIS-SPECTRAL PARAMETERS FOR RX J0136.9−3510

Model[a]	Γ	*kT* (eV)	E_L (keV)	EW (eV)	χ^2/dof
PL (2–8 keV)	$2.28^{+0.09}_{-0.10}$	...	...	...	120.3/127
PL (0.7–8 keV)	2.28 (fixed)	...	...	...	804.8/291
PL (0.7–8 keV)	$2.99^{+0.08}_{-0.07}$	...	...	...	458.8/290
PL+BB (0.7–8 keV)	$2.23^{+0.15}_{-0.08}$	153^{+18}_{-11}	...	...	386.8/288
PL+RS (0.7–8 keV)	$2.26^{+0.014}_{-0.08}$	198^{+27}_{-19}	...	...	385.1/288
PL+RS+GA (0.7–8 keV)	$2.27^{+0.14}_{-0.08}$	196^{+27}_{-18}	$5.89^{+0.12}_{-0.09}$	860^{+390}_{-413}	374.1/286

[a] The value of the hydrogen column density was fixed with the Galactic value (1.79×10^{20} cm^{-2}) plus an additional fixed absorption parameter ($N_H = 9.0 \times 10^{20}$ cm^{-2}) to compensate for the low-energy efficiency losses of the SIS detectors.

($kT_{BB} = 0.15 \pm 0.02$ keV) components (when added with the above model, with Γ being a free parameter equaling 2.2 ± 50.15) fit equally well with the soft excess emission component ($\Delta\chi^2 = 72$ for an addition of 2 dof, with an *F*-test value of 26.8 and a probability of 2.1×10^{-11}). The emission-line feature around 5.9 keV was modeled by adding a Gaussian component with the above model. The width of the line was fixed at 0.01 keV, and the line energy and strength were left free. The addition of the Gaussian component reduces the value of χ^2 by 11.0 for the addition of two free parameters, which suggests that an emission line is present in the spectrum of RX J0136.9−3510 at a level better than 98.4% (with an *F*-test probability of 1.6×10^{-2}). Results of the best-fit parameters are shown in Table 1. The observed equivalent width (EW) of the emission line is 860^{+390}_{-413} eV, and the observed and unabsorbed fluxes (0.7–8.0 keV range) are $(8.42 \pm 1.02) \times 10^{-13}$ and $(8.54 \pm 0.99) \times 10^{-13}$ ergs cm^{-2} s^{-1}, respectively. The corresponding luminosities are $(4.96 \pm 0.61) \times 10^{44}$ and $(5.04 \pm 0.61) \times 10^{44}$ ergs s^{-1}, respectively. The RS or the BB components contribute ~23% to the flux in the *ASCA* band. Figure 4 shows the data, combined model, model components, and the ratio between the data and the model. The overall fit of the spectra is poor mainly because of the calibration uncertainties of the SIS detectors at low energies.

4. DISCUSSION

Figure 1 displays the presence of extended soft X-ray emission in RX J0136.9−3510. The *ROSAT* HRI image shows uniform distribution of this extended component around the nucleus. Even though the *ROSAT* PSPC spectrum cannot distinguish between the thermal and nonthermal origin of this component, the soft excess component of the *ASCA* SIS spectra is best fitted with the thermal model. RX J0136.9−3510 is a bright Two Micron All Sky Survey source (Barkhouse & Hall 2001), and the derived 25–60 μm *IRAS* color of RX J0136.9−3510 is around 10^{-2}. Based on the observed X-ray flux and the *IRAS* color of this NLS1, it is suggested that a possible starburst component may be present in this object (Risaliti et al. 2000). Thus, with the existing data, it is suggested that the extended emission may be the remnants of the starburst activities in this NLS1. If this is true, then this result supports the suggestion that the starburst galaxies may be the parent population of NLS1s (Mathur 2000).

The observed 5.9 keV emission line corresponds to 7.6 keV at the source frame. This spectral feature may be either a highly blueshifted He-like (6.7 keV) or H-like (6.9 keV) Fe Kα line, which clearly indicates the presence of a relativistic outflow of matter in this NLS1. Outflows of material in a wide range of ionization states have been detected in nearby Seyfert galaxies, and it is believed that outflow may be a common phenomena in AGNs (Sako et al. 2001; Kaspi et al. 2002). However, relativistic outflow in contrast to jets is very rare in AGNs, even though such outflow was detected (velocity ~0.27*c*) in the Galactic sources like SS 433 (Kawai et al. 1989; Marshall et al. 2002). Recently, relativistic outflow has been detected in a few AGNs. For example, blueshifted highly ionized absorption lines of Fe and other elements have been detected in the gravitationally lensed quasar APM 08279+5255 with velocity in the range ~0.2*c*–0.4*c* (Chartas et al. 2002), in the luminous radio-quiet quasar PDS 456 at a velocity of ~0.17*c* (Reeves et al.

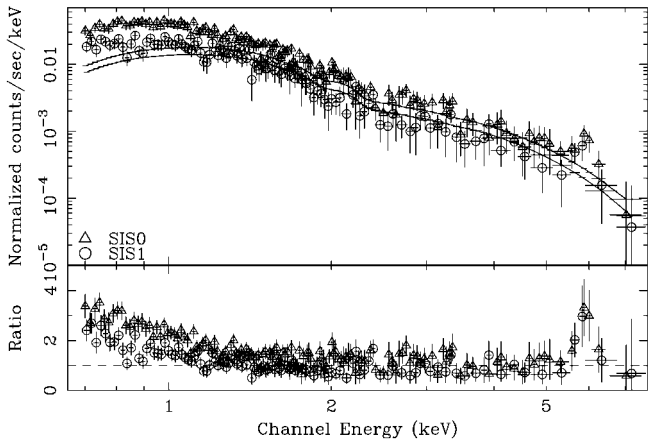

FIG. 3.—*ASCA* SIS0 (*triangles*) and SIS1 (*circles*) spectra and the model (GA-corrected power law with Γ = 2.3; *top panel*) and the ratio between the data and the model (*bottom panel*). The presence of an excess emission below 1.0 keV and an emission line around 5.9 keV at the observer's frame (7.6 keV at the source frame) can be seen.

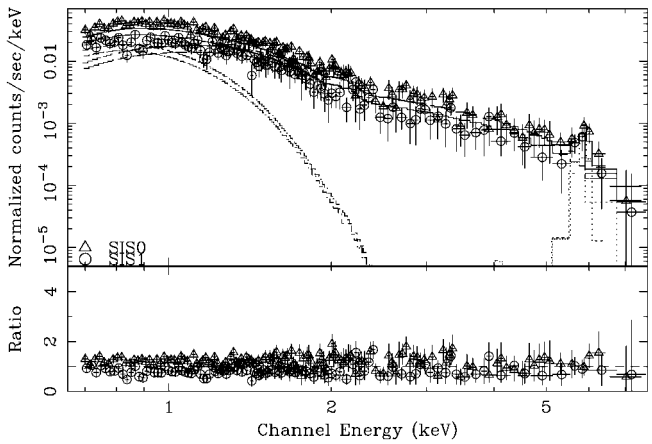

FIG. 4.—Same as Fig. 3, but for the GA-corrected RS+PL+Gaussian model.

2003), in the narrow-line radio-quiet quasar PG 0844+349 at a velocity of ~0.2*c* (Pounds et al. 2003a), and also in the NLS1 PG 1211+143 at a velocity of ~0.1*c* (Pounds et al. 2003b). In addition, a highly blueshifted Fe K emission line is seen in PKS 2149−306 (Yaqoob et al. 1999) and in the Seyfert-like galaxy CXOCDFS J033225.3−274219 with velocity of the order of 0.6*c*–0.7*c* (Wang et al. 2003). Thus, our detection of a highly blueshifted Fe K emission line in RX J0136.9−3510 is not unique but extremely important. With the *ASCA* spectrum, we are unable to determine the outflow velocity (~0.2*c* if the emission line is He-like or ~0.1*c* if it is H-like). He-like Fe Kα is in general much stronger than H-like Fe Kα in photoionized media (Nayakshin & Kallman 2001), whereas in collisionally excited plasma, the H-like component may become dominant (Bautista & Titarchuk 1999). The high blueshift of the line indicates formation in extreme outflows, which in principle is possible when the emission comes from distances much larger than the inner accretion disk radius, i.e., when the outflow runs into the extended emission region. Ionized accretion disk reflection may produce broad emission lines with large equivalent widths, but the lines will not be highly blueshifted (Nayakshin & Kallman 2001 and references therein). For the steep spectrum of RX J0136.9−3510 ($\Gamma = 2.27^{+0.14}_{-0.08}$), detection of a highly ionized Fe Kα line tentatively favors a concentration of the X-ray flux to small regions above the disk. Otherwise the predominant optical/UV/soft X-ray emission would cool the plasma to the point where it could not emit such highly ionized features. Thus, the present results indicate that, most likely, the observed emission line was formed in collisionally excited plasma as a result of the interaction of the outflow with a high-density ambient medium.

BALQs are strong Fe II and weak C IV and [O III] line emitters, like the NLS1s (Lawrence et al. 1997; Leighly et al. 1997). In addition, both BALQs and NLS1s have relatively strong IR continuum emission compared with the optical. All these properties have been observed in RX J0136.9−3510, and the detection of high-velocity outflow, which is common in BALQs, indicates that this NLS1 may be the low-redshift counterpart of BALQs (Brandt et al. 1999). Future high spatial resolution observations with *Chandra* will reveal the energy-dependent X-ray morphology of the extended emission and permit us to clearly identify the origin and nature of this extended emission component. Spectroscopic observations with *XMM* will allow us to detect and to study the blueshifted emission-line profile(s) of RX J0136.9−3510.

Our sincere thanks to S. Nayakshin for his valuable comments and suggestions on the spectral properties of RX J0136.9−3510. We are thankful to D. Grupe for providing us with his optical spectrum of RX J0136.9−3510. We are grateful to the anonymous referee for valuable suggestions.

REFERENCES

Balucinska-Church, M., & McCammon, D. 1992, ApJ, 400, 699
Barkhouse, W. A., & Hall, P. B. 2001, AJ, 121, 2843
Bautista, M. A., & Titarchuk, L. 1999, ApJ, 511, 105
Boller, T. 2000, NewA Rev., 44, 387
Boller, T., Brandt, W. N., Fabian, A. C., & Fink, H. H. 1997, MNRAS, 289, 393
Boller, T., Brandt, W. N., & Fink, H. H. 1996, A&A, 305, 53
Brandt, W. N., Boller, T., Fabian, A. C., & Ruszkowski, M. 1999, MNRAS, 303, L53
Brandt, W. N., & Gallagher, S. C. 2000, NewA Rev., 44, 461
Brandt, W. N., Mathur, S., & Elvis, M. 1997a, MNRAS, 285, L25
Brandt, W. N., Mathur, S., Reynolds, C. S., & Elvis, M. 1997b, MNRAS, 292, 407
Chartas, G., Brandt, W. N., Gallagher, S. C., & Garmire, G. P. 2002, ApJ, 579, 169
David, L. P., et al. 1995, The *ROSAT* High Resolution Imager (Cambridge: SAO)
Goodrich, R. W. 1989, ApJ, 342, 224
Grupe, D. 1996, Ph.D. thesis, Univ. Gottingen
Grupe, D., Beuermann, K., Mannheim, K., & Thomas, H.-C., 1999, A&A, 350, 805
Grupe, D., Beuerman, K., & Thomas, H.-C., Mannheim, K., & Fink, H. H. 1998, A&A, 330, 25
Kaspi, S., et al. 2002, ApJ, 574, 643
Kawai, N., Matsuoka, M., Pan, H.-C., & Stewart, G. C. 1989, PASJ, 41, 491
Kuraszkiewicz, J., Wilkes, B. J., Czerny, B., & Mathur, S. 2000, ApJ, 542, 692
Lawrence, A., et al. 1997, MNRAS, 285, 879
Leighly, K. M., et al. 1997, ApJ, 489, L25
Leighly, K. M., et al. 1999a, ApJS, 125, 297
———. 1999b, ApJS, 125, 317
———. 2000, NewA Rev., 44, 395
Marshall, H. L., Canizares, C. R., & Schulz, N. S. 2002, ApJ, 564, 941
Mathur, S. 2000, MNRAS, 314, L17
Mathur, S., Kuraszkiewicz, J., & Czerny, B. 2001, NewA, 6, 321
Nandra, K., et al. 1997, ApJ, 476, 70
Nayakshin, S., & Kallman, T. R. 2001, ApJ, 546, 406
Netzer, H. 2000, NewA Rev., 44, 477
Nicastro, F., Fiore, F., & Matt, G. 1999, ApJ, 517, 108
Nikolajuk, M., Papadakis, I. E., & Czerny, B. 2004, MNRAS, submitted (astro-ph/0403326)
Osterbrock, D. E., & Pogge, R. W. 1985, ApJ, 297, 166
Pounds, K. A., et al. 2003a, MNRAS, 345, 705
———. 2003b, MNRAS, 346, 1025
Puchnarewicz, E. M., et al. 1992, MNRAS, 256, 589
Reeves, J. N., O'Brien, P. T., & Ward, M. J. 2003, ApJ, 593, L65
Reeves, J. N., & Turner, M. J. L. 2000, MNRAS, 316, 234
Risaliti, G., et al. 2000, A&A, 357, 13
Sako, M., et al. 2001, A&A, 365, L168
Tennant, A. F., & Mushotzky, R. F. 1983, ApJ, 264, 92
Vaughan, S., Reeves, J., Warwick, R., & Edelson, R. 1999, MNRAS, 309, 113
Véron-Cetty, M.-P., Véron, P., & Gonçalves, A. C. 2001, A&A, 372, 730
Wang, J., et al. 2003, ApJ, 590, L87
Wills, B. J., et al. 1999, ApJ, 515, L53
Yaqoob, T., et al. 1999, ApJ, 525, L9
———. 2000, *ASCA* GOF, Calibration Memo, ASCA-CAL-00-06-01, Ver. 1.0 (http://heasarc.gsfc.nasa.gov/docs/asca/calibration/nhparam.html)
Zombeck, M. V., et al. 1995, Proc. SPIE, 2518, 304